International Journal of Heat and mass Transfer, Vol. 54 (2011) 2602–2608.

Prediction of thermal conductivity of steel

M. J. Peet[1*], H. S. Hasan[2] and H. K. D. H. Bhadeshia[1]

Published in the International Journal of Heat and Mass Transfer
Vol. 54 (2011) page 2602-2608
doi:10.1016/j.ijheatmasstransfer.2011.01.025

Abstract

A model of thermal conductivity as a function of temperature and steel composition has been produced using a neural network technique based upon a Bayesian statistics framework. The model allows the estimation of conductivity for heat transfer problems, along with the appropriate uncertainty. The performance of the model is demonstrated by making predictions of previous experimental results which were not included in the process which leads to the creation of the model.

Keywords: Thermal Conductivity, Steel, Bayes, Neural Network, Heat treatment, Mathematical models, Physical properties, Temperature, Commercial alloys, Matthiessen's rule

1 Introduction

There are many situations in design or in process modelling where it would be useful to know the thermal conductivity of the steel being used, and how it would change as a function of temperature. With the lack of any quantitative model the usual recourse is to look for a similar composition contained in published tables of data [1, 2, 3]. However, in the absence of a quantitative model it is not possible to assess the validity of this procedure.

Thermal conductivity controls the magnitude of the temperature gradients which occur in components during manufacture and use. In structural components subjected to thermal cycling, these gradients lead to thermal stresses. During heat treatment the conductivity limits the size of components that can be produced with the desired microstructure, since transformation depends on cooling rate and temperature. A suitable model of thermal conductivity should help to improve the design of steels and understanding of heat treatment, solidification and welding processes, design of steel structures and components, and prediction of thermo–mechanical fatigue.

The original motivation of the authors was to estimate thermal conductivity of a range of steels to assess the validity of lump–theory approximation in the design of a novel probe used to measure heat transfer coefficient [4, 5]. The model presented here was developed using neural network software to model the thermal conductivity

[1]http://www.msm.cam.ac.uk/phase-trans/
Department of Materials Science and Metallurgy, University of Cambridge, Pembroke Street, Cambridge, CB2 3QZ, UK.
[2]Department of Electromechanical Engineering, University of Technology, Baghdad, Iraq.

as function of composition and temperature. Subsequently the model was combined with experimentally determined heat transfer coefficient in a finite–element scheme to predict the instantaneous temperature profile in a cylinder of steel during quenching [4]. Calculated cooling curves and transformation kinetics were used to calculate the resultant distribution of hardness using a quench factor [6].

1.1 Thermal Conductivity

In metals electrons provide an additional contribution to the thermal conductivity, which can therefore be much greater than in non–metals in which only phonons contribute. Interactions between phonons and electrons determine the thermal conductivity in a pure metal. In alloys additional lattice distortions by alloying elements cause similar disturbances. Both relying on electron transport, thermal and electrical conductivity behave analogously, and in the ideal case are related by the Wiedermann–Franz law [7].

At temperatures above the Debeye temperature phonons begin to have wavelengths similar to the inter–atomic spacing and increasingly scatter electrons. For iron this is 398±9 or 418±4 K from X–ray measurements, or calculated to be 467 K from the elastic–constants [8]. The maximum thermal conductivity occurs at cryogenic temperatures. Due to phonon interactions the thermal conductivity is expected to decrease with increasing temperature, before this effect saturates and thermal conductivity becomes independent of temperature [9].

When an electron is deflected by an irregularity it changes quantum state. With more empty states available of similar energies there is a smaller mean free path and a greater chance that it will be deflected by a given irregularity. The resistance of alloys with the foreign atoms in solid solution is nearly always greater than that of a pure metal.

Matthiessen showed that in general the effect of alloying in dilute concentrations is independent of temperature [10]. Both the high resistance of alloys and Matthiessen's rule is explained by the electron interactions with the matrix. The resistance of a pure metal is largely due to the disturbance to the periodicity by thermal agitation. When foreign atoms are added they cause breaks in the lattice, and electrons will be deflected in the absence of thermal agitation. The electrical resistivity of the metal can be written as two separate components; $\rho = \rho_0 + \rho_T$. Such a relation has been demonstrated in a series of copper binary alloy [11], and according to Mott may be expected to be true only in dilute solid solutions [12].

Nechtelberger [13] related the change in thermal conductivity λ of ferrite in cast iron by alloying to the thermal conductivity of pure iron λ_0 by an equation of the form $\lambda = \lambda_0 - \ln \sum x$ where x is the solute concentrations in %.

Since there is a large effect on thermal conductivity by any disturbance in the periodicity of the lattice, the temperature and thermal history of steels can be expected to greatly influence conductivity. Without changing composition, a large number of different microstructures can be achieved, having different constituents, of different compositions and distributions. For example, quickly cooling a steel from the austenite range is likely to produce a martensitic microstructure, with carbon and other alloying elements present in a super–saturated solid solution of

metastable α'–ferrite. Heating will then trigger tempering behaviour, as carbides will precipitate and grow. In comparison cooling would produce a coarse mixture of cementite and ferrite of lower alloy content, and with lower defect density. The thermal conductivity of the martensite would be lower, and would increase towards that of the ferrite/cementite mixture on heat treatment below the austenite phase field. As temperatures increase into range 700–900°C and beyond the phonon contribution should become more dominant, also the phase change to austenite occurs and elements go into solution.

Richter [14] and Powell [15] have reported physical properties as a function of temperature for a number of different steels. The thermal conductivity of steel alloys diverge as temperature is decreased, pure iron having the highest thermal conductivity, followed by carbon steels, alloy steels and then by high–alloy steels. High–alloy steels having lower thermal conductivity at normal ambient temperatures than at high temperatures. At higher temperatures where austenite forms all the alloys have similar thermal conductivities.

Thermal conductivity of an alloy will depend upon temperature and microstructure (therefore time). In principle an accurate model should be possible when the microstructure can be accurately predicted. A law of mixtures rule could be successful in some cases, in other cases the distribution of phases will also be important. Cast irons have enhanced thermal conductivity due to the presence of graphite and it has been found by experience that the form of the graphite has a large influence. Flake graphite forms an interconnected network, whereas percolation is not possible with the stronger and more ductile nodular graphite form. Compacted graphite has intermediate properties, avoiding sharp edges of flake graphite, but still able to form a network structure.

2 Method

To investigate the composition dependence of the thermal conductivity a database was collated and a neural network produced in the Bayesian framework following MacKay [16, 17, 18, 19], as implemented in the bigback [20] program using the commercially available Neuromat [21] model manager software interface. In this scheme the neural network can be regarded as a general form of regression, providing an approach by which a quantitative prediction may be made in situations where the complexity of the problem makes a physically rigorous treatment difficult or impossible. This approach incorporates many techniques to automatically infer the relevance of the inputs and to avoid 'over–fitting', and has been successfully applied to many complex relationships in materials science [22, 23, 24, 25]. Bhadeshia has published two comprehensive reviews on their use and performance [26, 27].

A database of the thermal conductivity of steels was compiled from the published literature [1, 2, 14, 15, 28, 29, 30, 31, 32, 33]. Data is generally available in a form giving the chemical composition, temperature and heat treatment condition of the steel. Details of the initial condition of the steel have been omitted from this model so as to make it more generally applicable, this also avoids any complications which would be introduced from differences in experimental procedure used to determine the thermal conductivity reported. Any differences due to microstructure can be

regarded as being incorporated into the uncertainty which accompanies the predicted values.

The database contained 756 thermal conductivity values representing more than 100 different steels at various temperatures. For many of the steels thermal conductivity had been reported over a range of temperatures, whereas others were only associated with a room temperature measurement. Details of the inputs and the ranges for which data was available can be seen in table 1. The data and the model have also been made available online [34].

Figure 1 illustrates the range and the distribution of the variables plotted against the thermal conductivity. A cursory examination of the data for temperature versus thermal conductivity shows that there is a greater variation in thermal conductivity at lower temperatures. At higher temperatures thermal conductivity decreases in all the steels so the data converge. Due to the data source being a sample from commercial steels, rather than specifically designed combinatorial experiments, there is a greater spread in commonly used alloying elements. We should therefore expect higher quality predictions for elements such as carbon, manganese and silicon in comparison to copper or aluminium were fewer different levels were present in the data.

The database contained sporadic data for the usually small amounts of boron, nitrogen and zirconium but there was not a sufficient number of examples to model the action of these three inputs sufficiently. These elements are sometimes added purposefully and particularly nitrogen would always be expected to be present but seldom reported for air melted steels. It was therefore assumed that the usually small amount these elements do not have a large effect on the thermal conductivity of steels and the inputs were removed. Steels including these elements in small amounts were kept in the database used for training. Any effect resulting from the variation of these elements should therefore be reflected as larger uncertainty in the predictions. If the amounts vary systematically with the other inputs it is even possible that the effect would still be modelled successfully even though it cannot be separated from the other inputs.

The data were divided in to two groups, a training set and a testing set. Later additional data was collected so that the final model can be quantitatively assessed, otherwise it may be better to reserve some of the data for final testing.

In the ideal case the data would be a random sample from the input space, with each input changing independently. This is seldom the case for collated metallurgical data from the literature, data usually being available for a number of fixed compositions; in this case with temperature then varied. With sparse data there is an advantage in carefully selecting which of the data will be included in the training and the testing sets. It was found to be advantageous to ensure that each set contained a sample representative of the whole data, and that as many as possible different example compositions be present in only one of the sets.

In training each model a number of different sub–models are trained. These had between 1 and 25 hidden units and used 9 different random seeds which controlled the initial weights of each node, so as to ensure convergence from different positions in weight space. This meant a total of 225 initial conditions in each case, resulted in 163 sub–models being successfully trained in the final model (model C). Testing

Input	Minimum	Maximum	Average	Standard Deviation
Fe wt %	8.69	100	89.2	16.3
C wt %	0	1.22	0.29	0.26
Mn wt %	0	13.0	0.75	1.26
Ni wt %	0	63.0	3.52	8.39
Mo wt %	0	4.8	0.34	0.83
V wt %	0	3.0	0.08	0.31
Cr wt %	0	30.4	3.83	6.86
Cu wt %	0	0.69	0.032	0.10
Al wt %	0	11.00	0.14	1.15
Nb wt %	0	3.00	0.067	0.33
Si wt %	0	3.50	0.28	0.48
W wt %	0	18.50	0.48	2.76
Ti wt %	0	1.40	0.015	0.11
Co wt %	0	55.90	0.93	6.05
P wt %	0	0.044	0.014	0.015
S wt %	0	0.050	0.016	0.018
Temperature / °C	-200	1571	385	332
Conductivity / $Wm^{-1}K^{-1}$	10.9	83.8	33.6	11.7

Table 1: Summary of the database of steel thermal conductivities, all elements are in wt %.

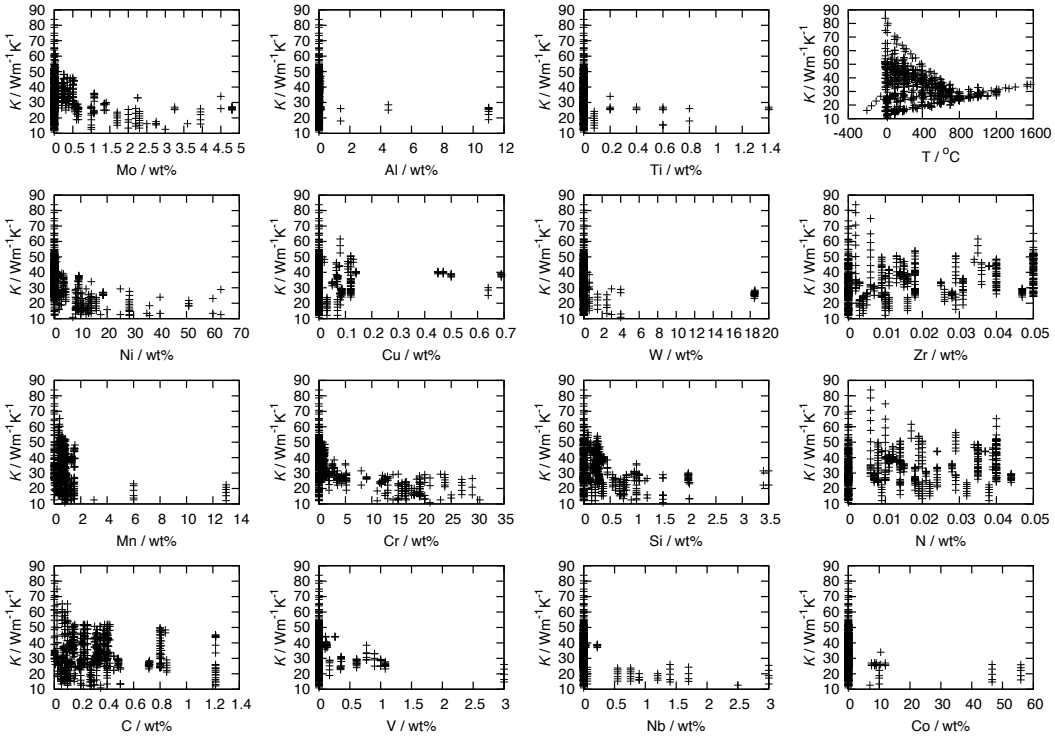

Figure 1: Distribution of inputs in the database.

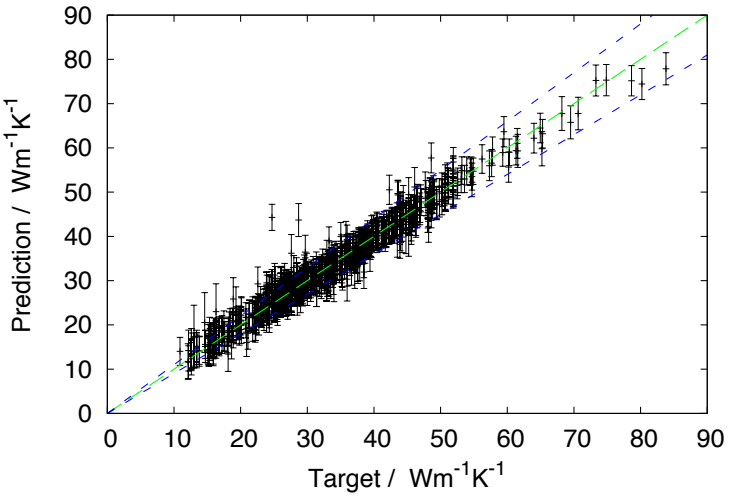

Figure 2: Comparison of experimental and calculated thermal conductivity for the committee model. Trend lines ±10% from the 1:1 correspondence illustrate the low scatter.

each of the sub–models capability to predict the unseen testing set, allows a ranking by the log predictive error. A committee of the best models as ranked by log–predictive–error (LPE) was selected to minimise the combined test error with seven sub–models found to be optimum in model C as shown in table 2. These models were allowed to further converge by training on the combined training and test data. As can be seen in figure 2 the final committee model can reproduce the training data, within the error bars estimated by the model for the vast majority of cases.

Before reaching the final database different combinations of inputs were attempted. The process of building a database, training and testing the neural network was repeated iteratively until reaching a satisfactory accuracy. The model can be quantitatively assessed by measuring the ability to predict data which has not been used in training the committee, as shown in table 3. In this case a large difference was observed in the confidence of predictions when each input was within the range seen in the database, compared to the case when one or more input was outside the range. The uncertainties correctly predicted the actual performance of each model.

Table 3 shows the improvement in the final few iterations of the model which used the full database described, this final testing is carried out using completely unseen data. Models A and B included an input for iron, derived as the balance of the other inputs. The difference between these two models is that the data was manually split between training and test sets in model A to ensure that conductivity data as a function of temperature for some of the alloys only appears in the training or the testing set. In model B the data was split randomly. Model A was found to perform better than model B, with lower error in predicting the unseen data, although model B had estimated a greater confidence in it's predictions.

In both model C and A the behaviour was safer in that the performance on the unseen data was slightly better than the perceived error by the model. Earlier in the development of the model it had been found that it was best to also include iron as an

Rank	LPE	TE	HU	Seed	Combined Test Error
1	569.05	0.485	4	4	0.486
2	568.76	0.481	4	6	0.484
3	566.90	0.491	4	3	0.486
4	566.22	0.918	9	2	0.440
5	562.01	0.749	7	9	0.397
6	559.22	0.558	3	8	0.403
7	558.88	0.500	6	9	0.395
8	558.79	0.575	3	4	0.403
9	558.66	0.555	3	1	0.410
10	555.80	0.560	4	7	0.412
11	554.70	0.549	4	5	0.419
⋮		⋮			⋮

Table 2: Model C ranking of sub–models by log–predictive–error (LPE). Sub–model's have varying number of hidden units (HU) and different random seeds, which determines the initial weights from which the model converges to an optimised solution. An optimum committee model can be produced from the best seven sub–models, so as to minimise the combined test error, lower than test error (TE) of the best model.

Model	Data set	Perceived accuracy σ_y	$rmse.$
A	Unseen data 'within range'	5.5	6.1
	Data beyond range	82.3	50.8
B	Unseen data 'within range'	5.2	12.1
	Data beyond range	65.4	51.5
C	Unseen data 'within range'	4.6	3.9
	Data beyond range	36.4	15.7

Table 3: Performance of model on unseen data. Unseen data was split into two groups because of the difference in performance in predictions, data was defined as 'within range' if each of the input values was within it's range in the database, due to the number of different permutations it is still possible to be extrapolating to completely unknown positions in the input space but for the data to be 'in range'.

input, however this has a risk of introducing an unnecessary bias. Therefore model C was trained excluding the iron input, this lead to an improvement in prediction for both data within the range of the inputs or when making predictions beyond the range of the inputs.

3 Results and discussion

Predictions for some of the alloys used to assess the model are shown in figures 3 and 4, the predictions compare favourably with the reference book and previous data from the literature. With the model reproducing the correct temperature dependence for the stainless steel, medium and high carbon steels. The compositions used are stated in the figure captions, each element is within the ranges shown in table 1.

During training the significance of each of the inputs is inferred from the data. These significances are shown in figure 5. The significance does not depend on how strongly each factor influences the output, but rather the complexity of the relationship. As could be expected temperature is one of the strongest influences, with high significance perceived by each of the sub–models. Manganese, nickel, molybdenum and chromium were observed to have a strong significance in most of the models. Carbon, silicon, vanadium and copper had a lower significance, while elements titanium, tungsten, niobium and aluminium all had very low significance. Except aluminium the elements with lowest significance are strong carbide formers, as such they may usually form second phases and so not effect the thermal conductivity greatly, except by removal of carbon or nitrogen. There is disagreement between the sub–models as to the significance of cobalt and sulphur, and these values varied widely between the different sub–models. The high significance of manganese, nickel and molybdenum may be related to their presence in stainless steels which will differ greatly from the majority of steels in the database, by stabilising austenite to low temperatures. It is surprising that carbon did not having the greatest significance due to it's strong effect on the transformation of austenite to ferrite, it may be due to the importance of the wide variety of heat treatments possible, of which no information has been included in the database. It seems that a feature of the model is a higher uncertainty of the thermal conductivity at lower temperatures, this reflects the greater number of microstructures that can present at low temperatures. Metastable microstructures will transform to become closer to equilibrium upon heating, this is reflected by the lower uncertainty in predictions at higher temperatures.

Figure 6 shows predicted thermal conductivities in some dilute solutions. It can be seen that the various alloying elements do not have equivalent effects, so Nechtelberger's equation for thermal conductivity of ferrite is not generally applicable. It can be seen that dilute solutions of manganese could be said to obey a thermal analog of Matthiessen's law below 1%, but the prediction for Fe-1% manganese deviated from linearity below around 300°C. If Matthiessen's law applies to thermal conductivity it can only be over a limited temperature range, since although the thermal conductivities of dilute solutions as a function of temperature could be approximately parallel and linear in the range 0–600°C the values for dif-

ferent compositions converge at higher temperatures. A transition occurs between 800–1000°C, to a different temperature dependence corresponding to the austenite phase, and with thermal conductivity increasing as temperature increases. However the predictions in this region are associated with larger uncertainties and it is not sensible to compare the effects of the various elements.

According to Farrell and Grieg [35] it is difficult to measure thermal conductivity better than 1% due to radiation effects, so in their careful measurements of thermal conductivity in nickel alloys they measured thermal conductivity between 2–100 K to see deviations from Matthiessen's rule. It seems likely that deviations observed at higher temperatures in the predictions of the neural network model are mainly due to phase–transformations, either precipitation or between ferrite and austenite. The perceived uncertainty of the prediction is much larger than 1%, however as observed in figure 4 the uncertainties encompass the experimental values and are similar order to the disagreement between the various studies of the thermal conductivity of the austenitic stainless steel, and also the non–linearity of thermal conductivity measurement of the ferritic stainless steel.

The model has some ability to extrapolate successfully, as can be seen in figure 7 the model can partly infer the behaviour at cryogenic temperatures, with reasonable match with experimental data [36] to -200°C which was the lowest temperature in the database. For pure iron the data was limited to above room temperature, as expected this data could be directly reproduced by the neural network. Beyond -200°C the thermal conductivity rapidly increases to a maxima at around -250°C before more strongly decreasing to near 0 as the temperature approaches absolute zero. Not being physically based and without any previous examples of this behaviour the neural network is not able to predict this behaviour, also as shown it is possible to make predictions beyond absolute zero which are not thought to have any physical meaning. This extrapolation to cryogenic temperatures was accompanied by an increase in uncertainty which contained all the experimental data until the temperature reached a few degrees Kelvin.

The model is naive in that it has no explicit knowledge of all the physical phenomenon which determine the thermal conductivity, the biggest omission is that no knowledge of the previous thermal history or microstructure was included. This was on one hand omitted to allow simple application of the model, secondly to simplify the modelling procedure, and thirdly to allow the greatest amount of data to be incorporated in the model. In reality the thermal conductivity will depend upon the microstructure of the steel, which depends upon the full thermal history of the steel, and may be also change during holding at a particular temperature. Where it is necessary to accounts for these effects, or when greater accuracy is needed than indicated by the uncertainty, experimental measurement of thermal conductivity would be required.

4 Conclusions

A general regression model has been created which is capable of predicting the thermal conductivity of steels as a function of composition and temperature. Since the neural network software applied automatically infers the relevance of the inputs,

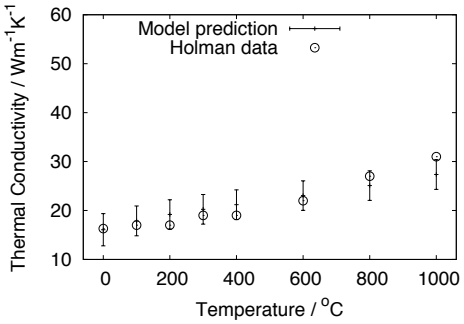

(a) 18Cr-8Ni wt% stainless steel (0.15C-0.25Mn-8Ni-18Cr wt%)

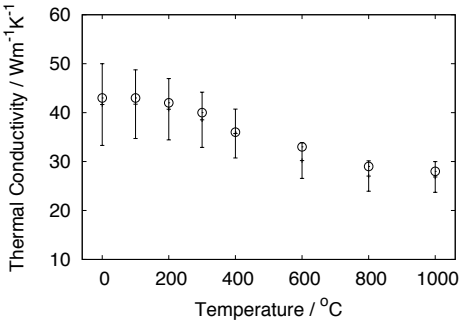

(b) 1C wt% steel (1C-0.5Mn-0.25Si wt%)

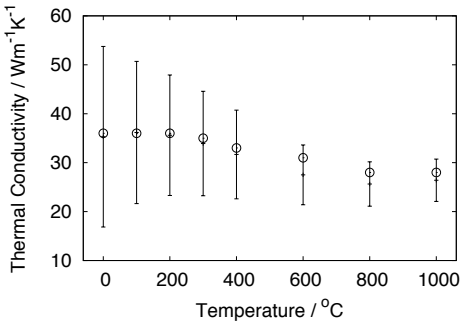

(c) 1.5C wt% steel (1.5C-0.5Mn-9,25Si wt%)

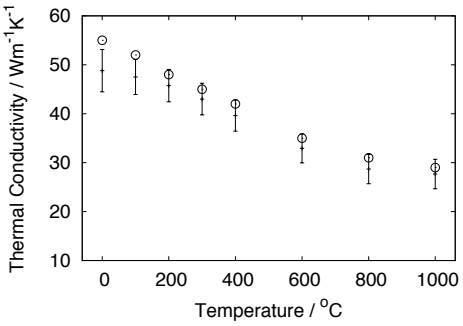

(d) 0.5C wt% steel (0.5C-0.5Mn-0.25Si wt%)

Figure 3: Predictions for unseen compositions, compared to experimental values (circles) [3].

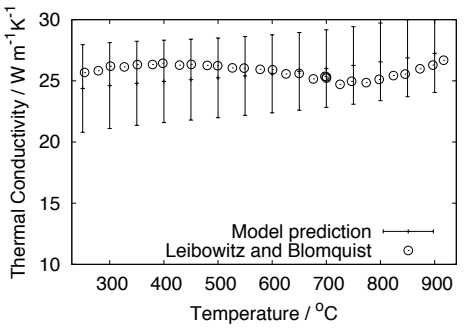

(a) HT9 ferritic stainless steel

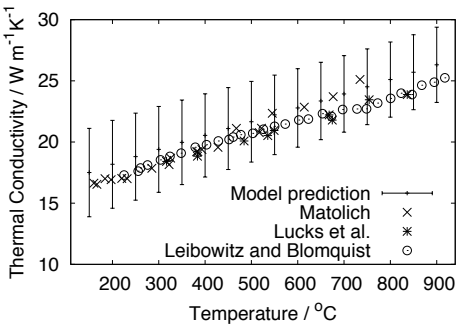

(b) D9 austenitic stainless steel

Figure 4: Comparison of predictions for unseen composition against experimental values from various authors [37, 38, 39].

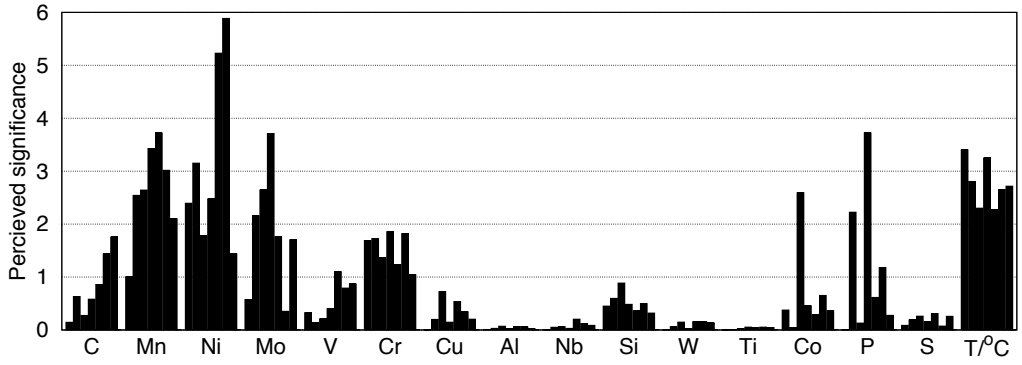

Figure 5: Significance of each input in each sub–model used to build the committee model, each element was included in weight percent.

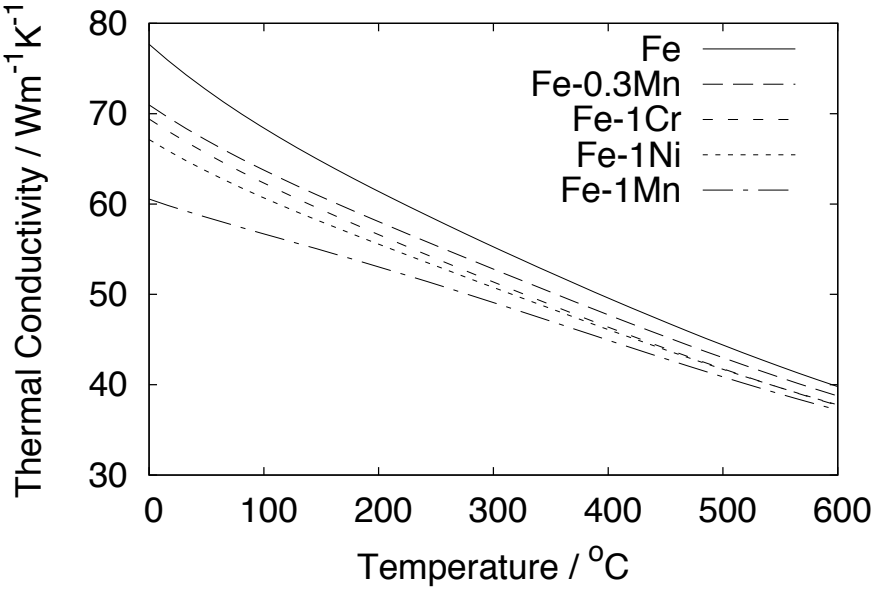

Figure 6: Prediction of the thermal conductivities of dilute solutions, uncertainties are omitted for clarity but are of order of ± 4.

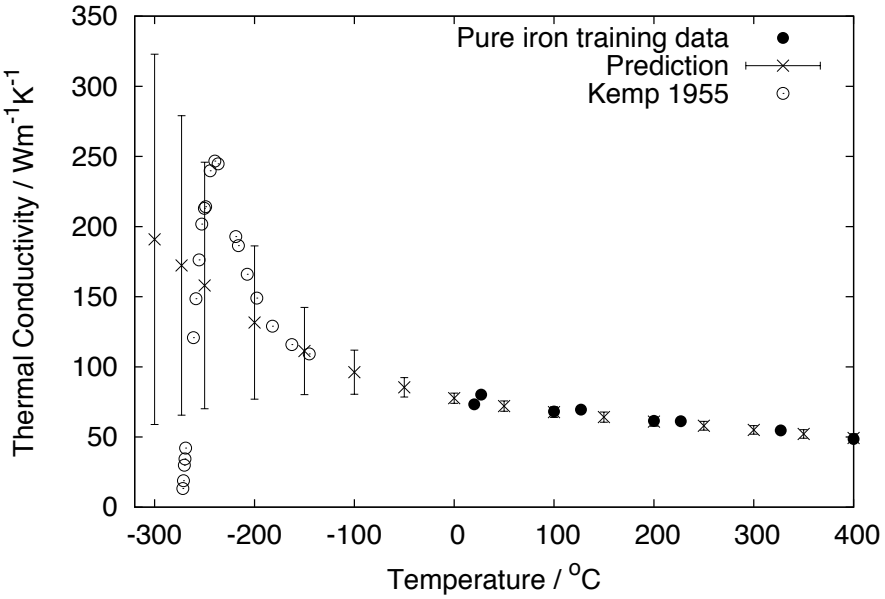

Figure 7: Prediction of the thermal conductivities of pure iron at cryogenic temperatures.

predictions can be made accompanied by appropriate uncertainties which vary with position in the input–space.

The model was tested on unseen data and can correctly predict the thermal conductivity for a wide range of steels.

5 Acknowledgments

The authors are grateful to the Iraqi Ministry of Higher Education and Rolls–Royce plc for funding and to Prof. A. L. Greer for provision of laboratory facilities.

References

[1] T. C. Totmeier W. F. Gale, editor. *Smithells Metals Reference Book*. Elsevier/ASM, 8 edition, 2004.

[2] Matweb website. http://www.matweb.com/, 2009.

[3] J. P. Holman. *Heat Transfer*. McGraw–Hill Companies, 1997.

[4] H. S. Hasan. *Evaluation of Heat Transfer Coefficients during Quenching of Steels*. PhD thesis, University of Technology, Baghdad, 2010.

[5] H. S. Hasan, M. Peet, J. M. Jalil, and H. K. D. H. Bhadeshia. Heat transfer coefficients during quenching of steels. *Heat and Mass Transfer*, 2010. DOI:10.1007/s00231-010-0721-4.

[6] J. T. Staley and J. W. Evancho. Kinetics of precipitation in aluminum alloys during continuous cooling. *Metall. Trans.*, 5:43–47, 1974.

[7] R. Franz and G. Wiedemann. *Ann. D. Physik*, 165(8):497–531, 1853.

[8] F. H. Herbstein and J. Smuts. Determination of Debeye temperature of α–iron by X–ray diffraction. *Philophical Magazine*, 8(87), 367–385 1963.

[9] N. F. Mott and H. Jones. *Theory of the Properties of Metals and Alloys*. Oxford University Press, 1958.

[10] A. Matthiessen and C. Vogt. *Ann. D. Phys. U. Chem.*, 122:19, 1864.

[11] C. Linde. *Ann. D. Physik*, 15:219, 1932.

[12] N. F. Mott. The electrical resistance of dilute solid solutions. *Mathematical Proceedings of the Cambridge Philosophical Society*, 32:281–290, 1936.

[13] E. Nechtelberger. The properties of cast irons up to 500°C. Technical report, Technicopy Ltd, 1980.

[14] F. Richter. *Die Wichtigsten Physikalishen Eigenschaften von 52 Eisenwerkstoffen*. Verlag Stahleisen GmbH, Dusseldorf, 1973.

[15] R. W. Powell and M. J. Hickman. Thermal conductivity of a 0.8% carbon steel. *Journal of the Iron and Steel Institute*, 154:112–116, 1946.

[16] D. J. C. MacKay. Bayesian non–linear modelling with neural networks. In H. Cerjak and H. K. D. H. Bhadeshia, editors, *Mathematical modelling of weld phenomena 3*. IOM, 1997.

[17] D. J. C. MacKay. *Bayesian methods for adaptive models*. PhD thesis, Caltech, 12 1991.

[18] D. J. C. MacKay. Bayesian interpolation. *Neural Computation*, 4(3):41, 1992.

[19] D. J. C. MacKay. A practical bayesian framework for backpropagation networks. *Neural Computation*, 4(3):448–472, 1992.

[20] bigback. URL:http://www.inference.phy.cam.ac.uk/mackay/bigback/.

[21] Neuromat's model manager. URL:http://www.neuromat.com/.

[22] T. Sourmail, H. K. D. H. Bhadeshia, and D. J. C. MacKay. Neural network model of creep strength of austenitic stainless steels. *Materials Science and Technology*, 18:655–663, 2002.

[23] H. K. D. H. Bhadeshia, D. J. C. MacKay, and L.-E. Svensson. Impact toughness of C–Mn steel arc welds - bayesian neural network analysis. *Materials Science and Technology*, 11:1046–1051, 1995.

[24] M. A. Yescas-Gonzalez, H. K. D. H. Bhadeshia, and D. J. C. MacKay. Estimation of the amount of retained austenite in austempered ductile irons. *Materials Science and Engineering A*, A311:162–173, 2001.

[25] R. C. Dimitriu and H. K. D. H. Bhadeshia. Hot-strength of creep-resistant ferritic steels and relationship to creep-rupture data. *Materials Science and Technology*, 23:1127–1131, 2007.

[26] H. K. D. H. Bhadeshia. Neural networks in materials science. *ISIJ International*, 39:966–979, 1999.

[27] H. K. D. H. Bhadeshia, R. C. Dimitriu, S. Forsik, J. H. Pak, and J. H. Ryu. On the perfomance of neural networks in materials science. *Materials Science and Technology*, 25(4):504–510, 2009.

[28] Efunda website. http://www.efunda.com/, 2009.

[29] Sandvik materials data sheets. http://www.dsmstaralloys.com/sandvik.htm.

[30] P. Kardititas and M-J Baptiste. Thermal and structural properties of fusion related material. http://www-ferp.ucsd.edu/LIB/PROPS/PANOS/ss.html.

[31] Bohler–Uddeholm materials data sheets. http://www.bucorp.com.

[32] G. F. Vander Voort, editor. *ASM Metals Handbook*, volume 1. ASM, 8 edition, 1999.

[33] Metal Ravne materials data sheets. http://www.metalravne.com.

[34] H. S. Hasan and M. J. Peet. Map data thermal. http://www.msm.cam.ac.uk/map/data/materials/thermaldata.html.

[35] T. Farrell and D. Grieg. The thermal conductivity of nickel and its alloys. *J. Phys. C. (Solid St. Phys.)*, 2(2):1465–1473, 1969.

[36] W. R. G. Kemp, P. G. Klemens, and G. K. Warren. Thermal and electrical conductivies of iron, nickel, titanium, and zirconium at low temperatures. *Australian Journal of Physics*, 9:180–188, 1955.

[37] L. Leibowitz and R. A. Blomquist. Thermal conductivity and thermal expansion of stainless steels D9 and HT9. *International Journal of Thermophysics*, 9(5):873–883, 1988.

[38] Jr J. Matolich. Report BAT-7096 (NASA-CR-54141). Technical report, Battelle Memorial Institute, 1965.

[39] C. F. Lucks, H. B. Thompson, A. R. Smith, F. P. Curry, H. W. Deem, and G. F. Bing. Technical report USAF-TR-6145-1. Technical report, United States Air Force, 1951.